INTERNATIONAL JOURNAL FOR NUMERICAL METHODS IN ENGINEERING
Int. J. Numer. Meth. Engng. **47**, 969–983 (2000)

Non-reflective planar boundary condition based on Gauss filter

Ruperto P. Bonet *, Norberto Nigro, Mario A. Storti and Sergio Idelsohn

Centro Internacional de Métodos Computacionales en Ingeniería (CIMEC), INTEC-(CONICET-UNL), Güemes 3450, 3000 Santa Fe, Argentina

SUMMARY

A non-reflecting boundary condition based on the Gauss filter is employed for the determination of scattered potential governed by the Helmholtz equation. A filtering layer is used for closing infinite domain calculations. An expression for the reflection coefficient is derived and an optimal filtering layer is designed. Numerical results validate the performance of this method for unbounded wave guide problems. Copyright © 2000 John Wiley & Sons, Ltd.

KEY WORDS: outgoing boundary condition; Helmholtz; filtering layer; scattering; Gauss filter; unbounded domain

1. INTRODUCTION

Numerous techniques are in use for the solution of acoustic wave radiation and scattering problems governed by the Helmholtz equation. A common feature to many of these methods is to get an approximate solution on a bounded domain. The papers by Givoli [1] and Moore *et al.* [2] provide good summaries of much of the work that has been done in this direction. Several non-local procedure has been developed in the last 10 years, such as the DtN method proposed by Givoli [3] and Giou and Keller [4] and developed by Harari and Hughes [5] and Harari *et al.* [6]. The DtN boundary condition is exact and non-reflecting at the continuum medium, but it is dependent of the operator and the dimensional space where this is defined, then, when you apply this boundary condition do you need to know the fundamental solutions in question.

A discrete non-local DNL method has been developed for the study of water waves radiation and scattering problems [7, 8] and for ship wave resistance problem [9].

A Gaussian filtering layer in rectangular co-ordinates is used to obtain non-reflecting boundary condition for unbounded wave guides in two dimensions, defining problems that can be solved by finite element method.

The Gaussian filter has a large utility in engineering applications. In image processing; for instance, the Gaussian outputs a 'weighted average' of each pixel's neighbourhood, with the

* Correpondence to: Ruperto P. Bonet, Grupo de Tecnologia Mecanica, INTEC, Güemes 3450, 3000 Santa Fe, Argentina. E-mail: rbonet@venus.arcride.edu.ar

Contract/grant sponsor: CONICET; contract/grant number: BID 802/OC-AR PID Nr. 26
Contract/grant sponsor: Universidad Nacional del Litoral (Argentina)

CCC 0029-5981/2000/050969–15$17.50

Received 4 September 1998
Revised 30 April 1999

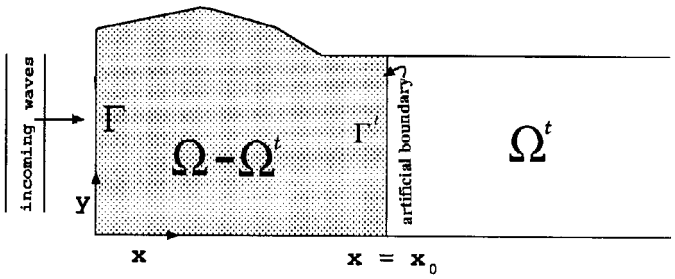

Figure 1. A model domain for radiation and scattering problem

average weighted more towards the value of the central pixel. Due to this fact, a Gaussian provides a gentle smoothing and preserves edges, and it attenuates high frequencies more than low frequencies. On the other hand, the Gaussian shows no oscillations.

Based on the Gauss filter, which is defined on the external region of the computational domain, we split the solution of the radiation problem governed by the planar Helmholtz equation, and obtain a novel non-reflective radiation boundary condition that characterize the 'outer' modes from the computational domain. The solution procedure is concerned to use standard finite element discretization in the computational domain, and in the external absorbing layer a linear system must be solved. The solution of this system is dependent of the parameters that characterize the absorbing layer, such that the thickness of the layer, the number of the layer points and the shape of the Gaussian filter.

In this paper we show that an infinite layer of this type can be used to solve the time harmonic radiation calculations. We also show that the truncated filtering layer reduces the reflection of the incident waves on the artificial boundary. In both cases an expression for the reflection coefficient is derived. Finally, we explain how to design the optimal filtering layers for scattering calculations, and how to use of the optimal parameters to solve a parallel plate wave guides with constant wavenumber. Such numerical results confirm the good performance of the Gaussian filtering method.

2. ORIGINAL PROBLEM AND REFORMULATION

The problem in question is to find the scattered wave produced when an incident wave is reflected from a scatterer. The mathematical problem is to find the solution to

$$\Delta\phi + k^2\phi = 0 \quad \text{in } \Omega \tag{1}$$

$$\phi = g \quad \text{in } \Gamma \tag{2}$$

$$\frac{\partial\phi}{\partial\mathbf{n}} = 0 \quad \text{on lateral boundaries} \tag{3}$$

$$+\,\text{some b.c.} \quad \text{at infinity} \tag{4}$$

where Ω is the unbounded domain and g is obtained from the incident wave. Γ is the location of the incoming wave front (Figure 1). The 'boundary condition at infinity' (4) guarantees the uniqueness of this problem. The basic idea for the reformulation of this problem on a bounded domain is to introduce an artificial boundary Γ^t and an appropriate boundary operator $\mathscr{B}$ that substitutes the

radiation condition at infinity. In this paper we consider a planar boundary $\Gamma^t = \{x = x_0\}$, which closes the computational domain $\Omega - \Omega^t$. This fact leads to the bounded boundary value problem on the $\Omega - \Omega^t$ region

$$\Delta\phi + k^2\phi = 0 \quad \text{in } \Omega - \Omega^t \tag{5}$$

$$\phi = g \quad \text{in } \Gamma \tag{6}$$

$$\frac{\partial\phi}{\partial\mathbf{n}} = 0 \quad \text{on lateral boundaries} \tag{7}$$

$$\frac{\partial\phi}{\partial\mathbf{n}} = \mathscr{B}\phi \quad \text{on } \Gamma^t \tag{8}$$

where $\mathscr{B}$ is still an unspecified boundary operator. This operator establishes a flux relation between ϕ and $\partial\phi/\partial\mathbf{n}$ on the artificial boundary Γ^t. For a given f on Γ^t, $\mathscr{B}\phi$ is defined as $\mathscr{B}f = \partial\psi/\partial\mathbf{n}$ where ψ is the solution of the semi-infinite parallel plate wave guide with $k = k_0$ constant wave number on the Ω^t semi-infinite domain, such that $\Omega^t = \{(x, y) \in \mathbb{R}^2 / x \geqslant x_0\}$

$$\Delta\psi + k^2\psi = 0 \quad \text{in } \Omega^t \tag{9}$$

$$\frac{\partial\psi}{\partial\mathbf{n}} = 0 \quad \text{on lateral boundaries} \tag{10}$$

$$\psi = f \quad \text{on } \Gamma^t \tag{11}$$

$$+ \text{some b.c.} \quad \text{at infinity} \tag{12}$$

In order to solve the unbounded problem (9)–(12), we substitute the radiation boundary condition (12) by a distributed radiation boundary condition on the Ω^t domain

$$\mathscr{L}(\psi) = \int_{x_0}^{\infty} \sigma(x)\psi e^{ikx}\, dx = 0 \tag{13}$$

where the $\sigma(x)$ kernel represents the shape of a Gaussian ('bell-shaped') hump, such that x_c parameter defines the centre of the bell, and s parameter defines the width of the bell

$$\sigma(x) = e^{-s^2(x-x_c)^2/2} \tag{14}$$

Finally, we solve analytically or numerically, problem (9)–(11) with condition (13) in the next sections.

3. AN EXACT GAUSS FILTER FOR HELMHOLTZ EQUATION IN UNBOUNDED DOMAIN

For simplicity, we consider the constant refraction index Helmholtz problem posed in a Ω^t half-plane (external region of the computational domain):

$$\Delta\psi + k^2\psi = 0 \quad (x \geqslant x_0,\ -\infty \leqslant y \leqslant \infty) \tag{15}$$

This equation admits solutions in the form of plane waves propagating at all angles $\theta = \theta_0$ relative to the x-axis, which can be expressed as follows:

$$\psi(x, y, \theta) = \hat{\psi}(x)e^{ik\sin\theta y} \tag{16}$$

Then, substituting (16) in (15) gives a one-dimensional problem

$$\frac{\partial^2 \hat{\psi}}{\partial x^2} + l^2 \hat{\psi} = 0, \quad x \geqslant x_0 \tag{17}$$

where $l = k\cos(\theta)$. We wish to choose a boundary condition at $x = x_0$ so as to minimize reflection of waves travelling towards the boundary from $x < x_0$. Considering incident waves of unit amplitude, we write $\hat{\psi}$ as

$$\hat{\psi}(x) = \mathrm{e}^{\mathrm{i}l(x-x_0)} + R\mathrm{e}^{-\mathrm{i}l(x-x_0)} \tag{18}$$

where R is the reflection coefficient. A boundary condition of the form

$$\hat{\psi}_x = \mathrm{i}l\hat{\psi}, \quad x = x_0 \tag{19}$$

produces the desired value $R = 0$ when (18) is substituted in (19), however, this boundary condition cannot generally be achieved [10], because it is neccesary to know the incident wave direction to the boundary in question. Several strategies have been reported to eliminate this difficulty in the past [1, 2, 4, 6]. Recently, Harari *et al.* [6] presented a derivation and the analysis of DtN formulations for unbounded wave guides in two and three dimensions. In virtue of this fact, the DtN operator is expressed in the form of infinite series. In contrast to them, in this paper, we introduce a novel strategy based on the Gauss filter, then a boundary condition is derived by means of the solution of unbounded problem (9)–(11), (13). A measure of the reflection of waves at the artificial boundary in virtue of the (13) 'distributed boundary condition based on Gauss filter' may be obtained by substituting (16) and (18) in (13). Then, the resulting reflection coefficient can be given as follows:

$$R = -\frac{\mathscr{L}(\mathrm{e}^{\mathrm{i}l(x-x_0)})}{\mathscr{L}(\mathrm{e}^{-\mathrm{i}l(x-x_0)})} \tag{20}$$

An estimate of the reflection coefficient can be given by the expression

$$R = -\frac{\tilde{\mathscr{L}}(\mathrm{e}^{\mathrm{i}lx})}{\tilde{\mathscr{L}}(\mathrm{e}^{-\mathrm{i}lx})} \tag{21}$$

provided that x_c be large enough and $\lambda \ll s \ll x_c$, such that

$$\tilde{\mathscr{L}}(\psi) = \int_{-\infty}^{+\infty} \mathrm{e}^{-s^2(x-x_c)^2/2} \psi \mathrm{e}^{\mathrm{i}kx}\, \mathrm{d}x$$

where λ denotes one wavelength. After some computation in (21) for an infinite layer, we obtain that the reflection coefficient modulus $|R|$ is independent of x_0 and x_c values, and it takes the form

$$|R| = \mathrm{e}^{-2kl/s^2} \tag{22}$$

We recall that this expression is independent of the position of the artificial boundary $x = x_0$ and the bell centre x_c, because they appear in the factor $\mathrm{e}^{2\mathrm{i}l(x_0-x_c)}$, of complex argument. Figure 2 shows the curves of reflection coefficient ($|R|$ in Db) versus the angle of incidence, for several s values of infinite layer. In this figure, we note that the reflection coefficient decreases for decreasing s values. In the following, we analyse the effect of truncation of this layer and we will show that there is an optimal s value for a discrete finite layer.

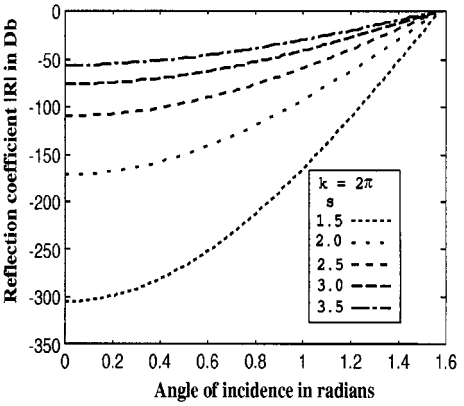

Figure 2. Reflection coefficient $|R|$ in Db (ie. $20\log_{10}|R|$) versus angle of incidence in radians

4. DISCRETIZATION OF THE PLANAR FILTERING LAYER

Next, we will investigate the effects of discretization on the one-dimensional finite layer. We consider only the Cartesian absorbing truncated layer, since in this case, we can compute the reflection coefficient directly. We consider the following problem:

$$\frac{\partial^2\hat{\psi}}{\partial x^2} + l^2\hat{\psi} = 0 \quad \text{in } x_0 \leqslant x \leqslant \delta \tag{23}$$

$$\hat{\psi} = g \quad \text{on } x = x_0 \tag{24}$$

$$\int_{x_0}^{\delta} \sigma(x)\psi e^{ikx}\,dx = 0 \tag{25}$$

on the absorbing truncated layer, located at the external region from the computational domain ($x \geqslant x_0$). This problem is discretized using the finite element method. We consider a uniform mesh, with element size h, so that the nodes are located at $x_j = jh$, $j = -1, 0, 1, 2, 3, \ldots, n_j$. x_0 is the node corresponding to the artificial boundary Γ^t. We denote $\delta = n_j h$ the layer thickness. We suppose that the term $\sigma^j = \sigma(x_j)$ is the function value of

$$\sigma(x_j) = \begin{cases} e^{-s^2(x_j - x_c)^2/2} & \text{for } 0 \leqslant j \leqslant n_j \\ 0 & \text{for } j < 0 \end{cases}$$

Here x_c is the bell centre. Using the finite element method to discretize problem ((23)–(25)), we obtain a linear equation system. For each l, a modal amplitude equation is expressed as follows:

$$a^j\hat{\psi}^{j-1} + b^j\hat{\psi}^j + a^j\hat{\psi}^{j+1} = 0 \tag{26}$$

where

$$a^j = 1 + \frac{l^2}{6} \tag{27}$$

$$b^j = -2 + \frac{2l^2}{3} \tag{28}$$

and $\hat{\psi}^j$ as the nodal potential values that satisfies the equation:

$$\mathscr{L}^h(\hat{\psi}) = \sum_{j=1}^{j=n_j} \sigma(x_j)\hat{\psi}^j \mathrm{e}^{\mathrm{i}kx_j} h_j = 0 \tag{29}$$

Let

$$\mathbf{U} = (\hat{\psi}^0, \hat{\psi}^1, \ldots, \hat{\psi}^{n_j})^{\mathrm{T}}$$

then

$$\mathbf{AU} = \mathbf{B}$$

where $\mathbf{A}$ is the $(n_j + 1) \times (n_j + 1)$ matrix defined by

$$\mathbf{A} = \begin{bmatrix} b^0 & a^0 & 0 & \cdots \\ a^1 & b^1 & a^1 & \cdots \\ & \ddots & \ddots & \ddots \\ \sigma^0 \mathrm{e}^{\mathrm{i}kx_0} & \sigma^1 \mathrm{e}^{\mathrm{i}kx_1} & \cdots & \sigma^{n_j} \mathrm{e}^{\mathrm{i}kx_{n_j}} \end{bmatrix}$$

and

$$\mathbf{B} = \begin{bmatrix} -a^0 \hat{\psi}^{-1} \\ 0 \\ \vdots \\ 0 \end{bmatrix}$$

We note that the $\mathbf{A}$ matrix is not sparse, due to the presence of the 'discrete distributed condition' at the last row, however, a strategy to solve this system while keeping the sparsity of this matrix can be easily implemented. Given that $\mathbf{B}$ is proportional to $\hat{\psi}^{-1}$, we can compute the solution in the form

$$\mathbf{U} = \left(\hat{\psi}^{*^0}, \hat{\psi}^{*^1}, \ldots, \hat{\psi}^{*^{n_j}} \right)^{\mathrm{T}} \hat{\psi}^{-1}$$

and a new condition is obtained on $\hat{\psi}^0$, $\hat{\psi}^1$

$$\hat{\psi}^{*^0} \hat{\psi}^1 - \hat{\psi}^{*^1} \hat{\psi}^0 = 0 \tag{30}$$

This condition is dependent of the propagation mode l and the parameters s, x_{c} that characterize the Gaussian filter. A boundary condition for the modal equation (17) can be expressed by the following relation:

$$\hat{\psi}^1 = \frac{\hat{\psi}^{*^1}}{\hat{\psi}^{*^0}} \hat{\psi}^0 \tag{31}$$

The above relation is called 'discrete local planar Gauss filter' boundary condition. We recall that this RBC is dependent of the kh dimensionless wavenumber and the incidence angle θ to the boundary $x = x_0$. Then, by means of this procedure, we can obtain the 'discrete planar Gauss filter' boundary condition for the two-dimensional problem in a diagonal basis.

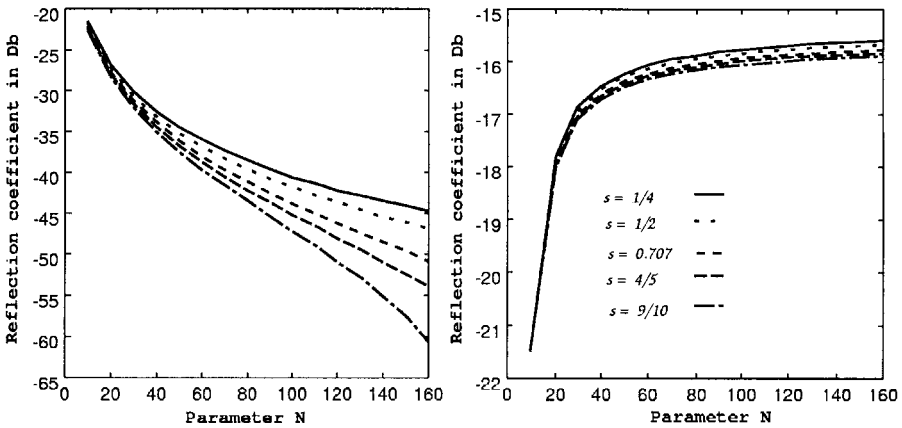

Figure 3. Numerical reflection coefficient at normal incidence (left) and $\theta = \pi/4$ rad (right)(in Db, i.e. 20 $\log_{10}$ $|R|$) versus the number of points per wavelenghts for five different values of s

5. DISCRETE REFLECTION COEFFICIENT

Next we examine the behaviour of the discrete local planar Gauss filter boundary condition (30). Based on the solution of the system

$$\begin{aligned} \hat{\psi}^0 &= (\hat{\psi}^+)^0 + (\hat{\psi}^-)^0 \\ \hat{\psi}^1 &= (\hat{\psi}^+)^0 \exp(+\mathrm{i}l^{(0)}h) + (\hat{\psi}^-)^0 \exp(-\mathrm{i}l^{(0)}h) \end{aligned} \tag{32}$$

we obtain the $(\hat{\psi}^+)^0$ and $(\hat{\psi}^-)^0$ wave field, the 'forward' and 'backward' wave field, respectively. Then, using (30) the discrete reflection coefficient for this layer is given by

$$|R| = \left| \frac{\hat{\psi}^{*1} - \exp(+\mathrm{i}l^{(0)}h)\,\hat{\psi}^{*0}}{\hat{\psi}^{*1} - \exp(-\mathrm{i}l^{(0)}h)\,\hat{\psi}^{*0}} \right|_{x_0} \tag{33}$$

In Figure 3 we show the variation of the numerical reflection coefficient $|R|$ versus the number of points per wavelength $N = 2\pi/kh$ for two different angles of incidence ($\theta = 0$ and $\theta = \pi/4$). We can observe that the scheme is consistent and the numerical reflection coefficient converges better for the angle of incidence 45°. For $\theta = 0$, note that the reflection coefficient decreases as the number of points in the layer increases. Convergence is faster for $\theta = \pi/4$. Finally, we remark that, when N is fixed, the smallest reflection coefficient is not necessarily obtained for the smallest value of s (Figure 4).

6. OPTIMIZATION OF THE CARTESIAN DISCRETE GAUSS FILTER

The optimization process is dependent on the number of points in the layer n_j, the number of points per wavelengths N and the parameters of the planar discrete Gauss filter, s and x_c. We consider that x_c is constant for all transversal modes, taken at the middle of the layer.

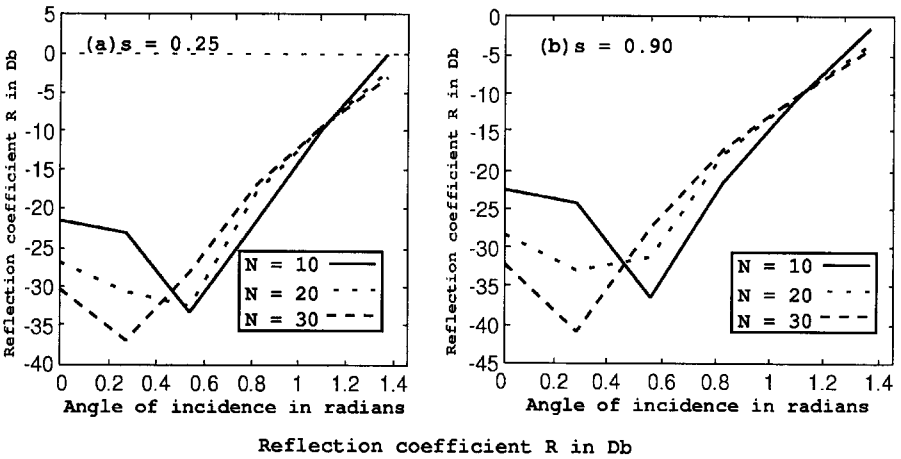

Figure 4. Numerical reflection coefficient (in Db, i.e. 20 $\log_{10}$ $|R|$) versus the angle of incidence for three different values of the number of points per wavelengths ($N = 10, 20, 30$). (left)$s = 0{\cdot}25$, (right)$s = 0{\cdot}9$

Analogously to Collins and Monk [11], we assume that the number of points in the layer n_j and the number of points per wavelengths N are fixed. In contrast with them, we look for a particular family of parameters, which provide the optimal ones such that the vector $\tilde{\sigma}$ defined by the layer, causes the lowest reflection coefficient. We decide to choose $\tilde{\sigma}$ in order to minimize R for all the progressive transversal modes m defined by the discretization. To compute an optimal layer $\left(h\tilde{\sigma}^0, h\tilde{\sigma}^1, \ldots, h\tilde{\sigma}^{n_j}\right)$, we minimize

$$\frac{1}{(M+1)} \sum_{m=0}^{M} |R_m(\theta_m, s)|^2 \cos(\theta_m) \tag{34}$$

over $(h\sigma^0, h\sigma^1, \ldots, h\sigma^{n_j})$. Here M is the number of progressive modes. Figure 5 shows several optimized standard layers for different thickness and parameters family. These layers have been obtained for a resolution of 20 points per wavelength in the $+x$ direction.

We can see that as the layer thickness increases, the optimal normalized Gauss filter curve on the layer (made non-dimensional to width length) gets narrower. In Table I we show the corresponding optimal values for each layer thickness (in wavelengths). These values have been obtained for $M = 99$. Reflection curves for several number of points per wavelength N for the layer thickness of one wavelength are shown in Figure 6. It can be seen that the process is convergent. Results of this computation for several thicknesses are shown in Figure 7. As expected, the upper envelope of the reflection coefficient curves for a given angle decrease as the width of the filtering layer increases (except for certain angles where the reflection goes to zero). For practical purposes the optimal value for s can be fitted as

$$s \sim 3{\cdot}2\delta^{-0{\cdot}45} \tag{35}$$

for layer widths of up to 10 wavelengths.

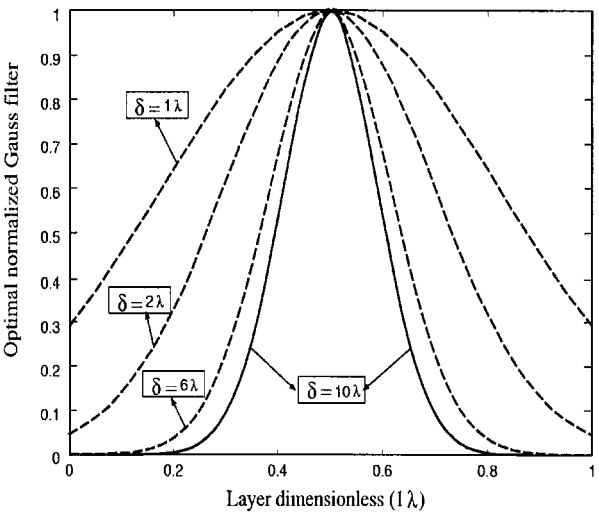

Figure 5. Optimal discrete normalized Gauss filter

Table I. Optimal filtering layer

Layer thick (λ)	Optimal s value	Average R
1	3·1430	2·7775e − 03
2	2·4905	1·3249e − 03
3	1·9199	2·7755e − 04
4	1·7823	2·8770e − 04
5	1·5157	9·6061e − 05
6	1·4585	1·1577e − 04
7	1·2935	4·5070e − 05
8	1·2638	5·8650e − 05
9	1·1472	2·4434e − 05
10	1·1229	3·0625e − 05

7. IMPLEMENTATION DETAILS

A radiation boundary condition based on the Gaussian filter is incorpored into finite element computation for a two-dimensional wave guide problem via the Galerkin form of the boundary-value problem (5)–(8). The solution procedure is concerned to use standard finite element discretization in the computational domain $\Omega - \Omega^t$, and in the external absorbing layer a linear system $\mathbf{AU} = \mathbf{B}$ must be solved, where the thickness of the layer δ, number of layer points n_j, the bell parameters x_c and s are chosen as described in Sections 5–7. From a practical viewpoint, we solve the discrete eigenvalue problem determined by $\mathbf{M}$ and $\mathbf{K}$ global matrices, in the expression $(1/h^2)\mathbf{M}^{-1}\mathbf{K} = \mathbf{V}\Lambda\mathbf{V}^{-1}$, where $\mathbf{V}$ is the eigenvector matrix, and Λ is the eigenvalue diagonal matrix. By means of $\mathbf{V}$ we obtain a decoupled linear equation system $\mathbf{AU} = \mathbf{B}$, in which, the matrix $\mathbf{A}$ is not sparse. To avoid this difficulty, we substitute the last row in the

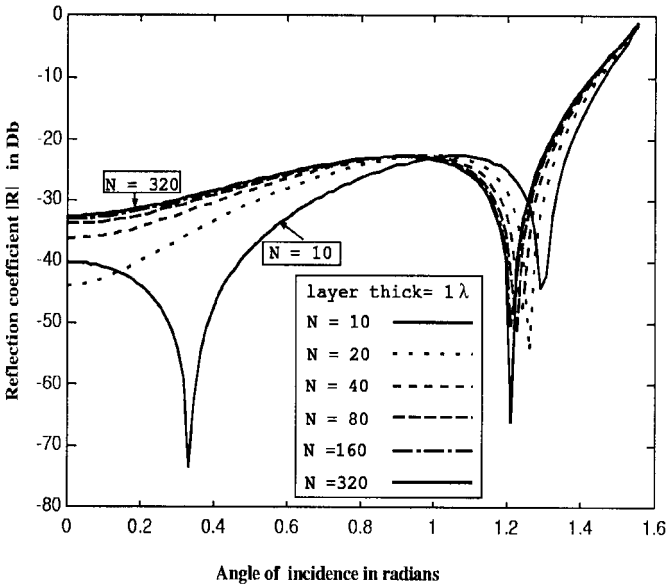

Figure 6. Optimal numerical reflection coefficient (in Db, i.e. 20 $\log_{10}|R|$) versus angle of incidence in radians, for several number of points per wavelengths

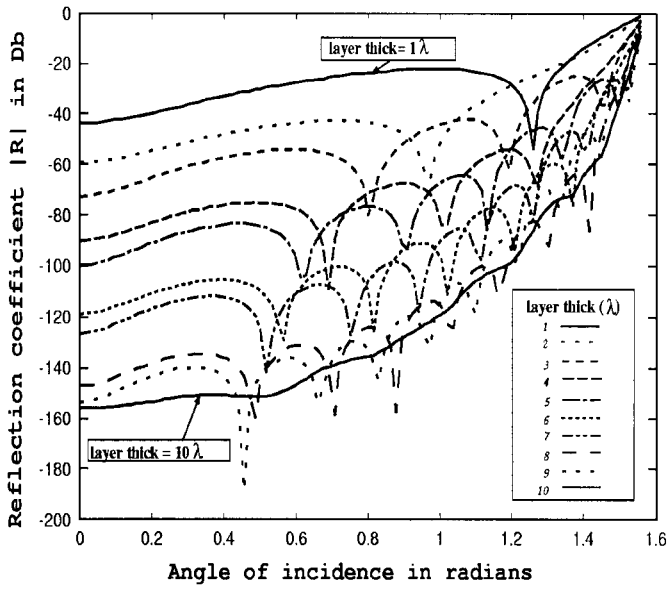

Figure 7. Optimal numerical reflection coefficient (in Db, i.e. 20 $\log_{10}|R|$) versus angle of incidence in radians, for several layer thickness (in wavelengths)

matrix by the row vector $[-1/h\ \ 1/h\ \ 0\ldots0]_{(n_j+1)}$. Then, we solve two linear equation systems $\mathbf{AU}=\mathbf{B}$, with the same matrix $\mathbf{A}$ and two linearly independent $\mathbf{B}$ vectors, hence the ψ_1 and ψ_2 solutions are linearly independent. Finally the solution of the problem is

$$\hat{\psi}^*(x_1,x_2,\ldots,x_{n_j})=\mathscr{L}^h(\psi_2)\psi_1-\mathscr{L}^h(\psi_1)\psi_2$$

and the local planar discrete Gaussian filter boundary condition takes the form (30). After that, taking $\mu_j=\hat{\psi}^*(x_1)/\hat{\psi}^*(x_0)$ value for each eigenvalue, and forming the matrix $G=\mathrm{diag}(\mu_1(\lambda),\ldots,\mu_{n_j}(\lambda))$, by means of the $\mathbf{V}$ matrix, we obtain the non-local Gauss filter boundary condition

$$\psi^1=\mathbf{F}\psi^0$$

where

$$\mathbf{F}=\mathbf{VGV}^{-1}$$

This boundary condition is incorporated to global level in the assembled stiffness matrix, and its contribution couples all of the degrees of freedom on the artificial boundary.

8. NUMERICAL RESULTS

We develop a numerical tests to show the performance of the boundary condition based on the Gaussian filter in various wave guide configurations. We seek a two-dimensional unbounded wave guide of constant width b, with Neumann wall conditions. A varying Dirichlet boundary condition which satisfies the wall conditions $\frac{1}{2}-(3737/18)(y/b)^2+(1{\cdot}0675/9)(y/b)^3-(21764/9)(y/b)^4+(18896/9)(y/b)^5-(1984/3)(y/b)^6$ is specified on the boundary at $x=0$, to excite significant contributions to the first three cross-sectional modes. A computational domain, determined by selecting $x_0=b/4$, is meshed with 20×20 bilinear rectangles. We employ this problem to compare the discrete non-local planar Gaussian filter boundary condition to known boundary conditions: the Sommerfeld condition and the planar DNL boundary condition. The real parts of the numerical results for $kb=2$ and 4 are compared to the analytical solution in Figures 8 and 9. Another numerical solutions for $kb=4$ case have been presented by Harari *et al.* [6] using the DtN method.

In both figures, we note the good correspondence between the numerical solution by the Gaussian filter condition and the analytical solution, improving the solution when the layer thickness increases. Also, we note that the Sommerfeld condition provides poor results. These results confirm that the planar Gaussian filter condition is not better than planar DNL boundary condition.

The effect of the Gaussian filter truncated boundary condition at the artificial boundary $x=x_0$ is shown in Figures 10 and 11 for the same wave numbers as in the above figures. The relative error

$$E=\frac{|\psi^h-\psi|_{x=x_0}}{|\psi|_{x=x_0}}$$

for the wave numbers $kb=2$ and 4 are shown in Figures 10 and 11, respectively. In general, we can observe that the error decreases as the layer thickness increases, until it reaches a given thickness value. The relative errors for $\delta=10$ or 20 are lower than 10 per cent. This demonstrates the good performance of this method.

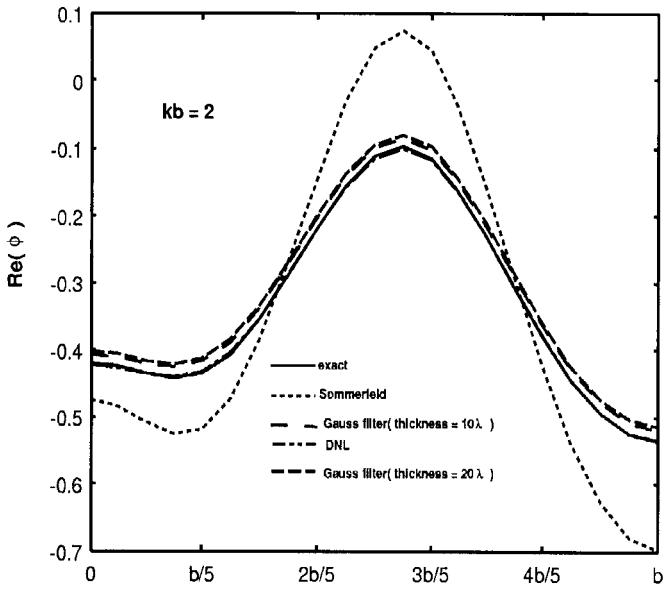

Figure 8. Comparison of boundary conditions along the artificial boundary, for $kb = 2$

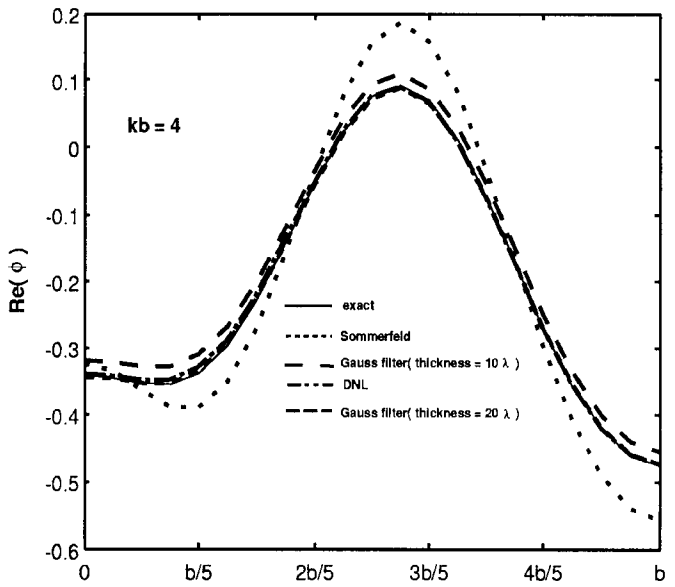

Figure 9. Comparison of boundary conditions along the artificial boundary, for $kb = 4$

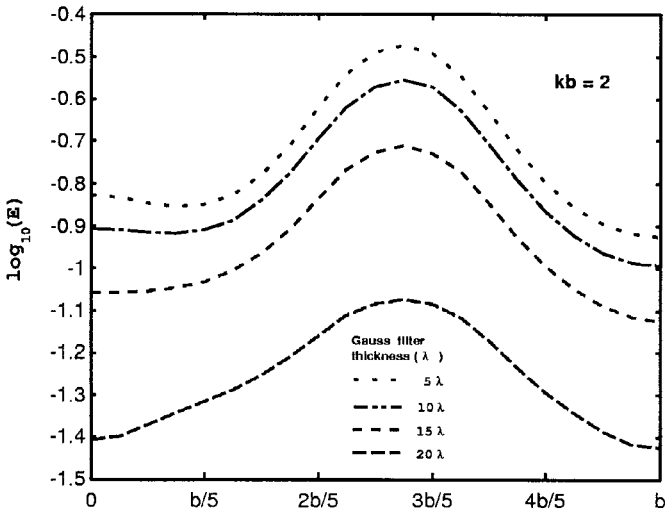

Figure 10. Dependence of the relative error on the layer thickness, for $kb = 2$

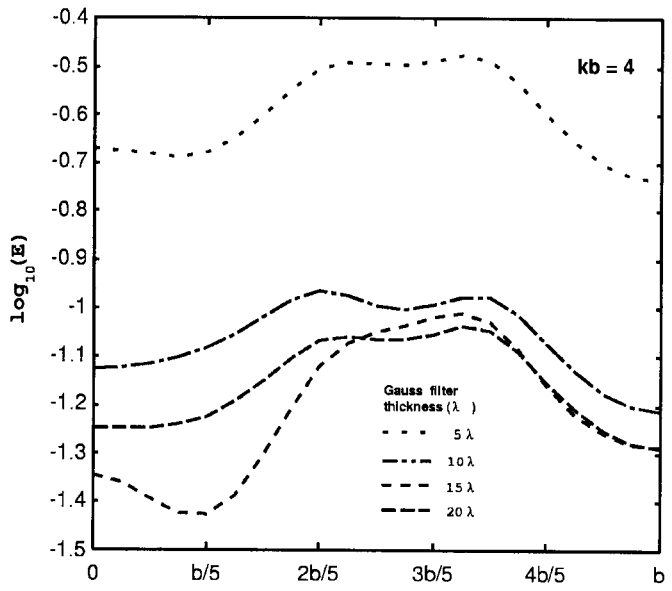

Figure 11. Dependence of the relative error on the layer thickness, for $kb = 4$

9. CONCLUSIONS

In this paper a strategy to solve wave problems numerically in unbounded domain by means of the Gauss filter for the planar Helmholtz equation is presented. By this procedure, a perfectly

absorbent boundary condition can be obtained on an infinite layer. For a finite layer, the solution procedure is that in the computational domain the standard finite element discretization is used, and in the exterior absorbing layer, the linear system $\mathbf{AU} = \mathbf{B}$ is solved, where the thickness of the layer δ, number of layer points n_j, and the bell parameters x_c and s are given. The truncation of this layer produces some reflections, and a procedure to get the optimal discrete Gauss filter has been developed. The optimal numerical reflection coefficient as function of layer thickness and the numerical resolution has been obtained. A regression law for the computation of the optimal s values is presented. Numerical results for a two-dimensional wave guide problem with constant wave number validate the good performance of this method.

APPENDIX

Nomenclature

$\mathscr{B}$	boundary operator
Δ	Laplacian operator
k_0	$2\pi/L_0$ constant wave number
k	$2\pi/L$ wave number
θ	angular polar co-ordinate
Ω	unbounded domain
$\Omega - \Omega^t$	finite element computation domain
Ω^t	outside the computation domain
i	$\sqrt{-1}$ imaginary unit
Γ	boundary surface (at the wave front)
Γ^t	artificial boundary
g	prescribed datum from the incident wave
h	water depth
L	wavelength
L_0	wavelength of wave front
ω	wave angular frequency
n	outward normal on boundary
C	wave celerity
T	wave period
ϕ	velocity potential values
ϕ^+	velocity potential values (forward component)
ϕ^-	velocity potential values (backward component)
ψ	velocity potential values in the unbounded problem
$\dot{\phi}$	derivate of ϕ with respect to x
$\mathbf{A}$	system matrix
$\mathbf{U}$	solution vector
$\mathbf{B}$	independent term matrix
$\mathbf{M}$	mass assembled matrix
$\mathbf{K}$	stiffness assembled matrix
j	layer index
δ	layer thickness

N number of points per wavelength in the layer
M transversal mode number
λ wavelength
R reflection coefficient
n_j number of nodes in the layer
σ Gaussian distribution
$(\mathscr{L})$ integral operator for the Gauss filter (in semi-infinite region)
$\tilde{\mathscr{L}}$ integral operator for the Gauss filter
σ Gaussian distribution
x_c bell centre
$1/S$ deviation
$\tilde{s}$ estimated s value

ACKNOWLEDGEMENTS

This work has received financial support from Consejo Nacional de Investigaciones Científicas y Técnicas (CONICE), Argentina) through grant BID 802/OC-AR PID Nr. 26, and from Universidad Nacional del Litoral (Argentina). We made extensive use of software distributed by the Free Software Foundation/GNU-Project: Linux ELF-OS, Octave, Tgif, Fortran f2c compiler and others.

REFERENCES

1. Givoli D. Non-reflecting boundary conditions: a review. *Journal of Computational Physics* 1991; **94**:1–29.
2. Moore TG, Glaschak JG, Taflove A, Kriegsmann GA. Theory and application of radiation boundary operators. *IEEE Transactions on Antennas and Propagation* 1988; **36**:1797–1811.
3. Givoli D. *Numerical Methods for Problems in Infinite Domains*, *in Studies in Applied Mechanics*, vol. 33. Elsevier: Amsterdam, 1992.
4. Givoli D, Keller JB. Non-reflecting boundary conditions for elastic waves. *Wave Motion* 1990; **12**:261–279.
5. Harari I, Hughes TJR. Studies of domain-based formulations for computing exterior problems of acoustics. *International Journal for Numerical Methods in Engineering* 1994; **37**:2935–2950.
6. Harari I, Patlashenko I, Givoli D. Dirichlet-to-Neumann Maps for unbounded wave guides. *Journal of Computational Physics* 1998; **143**:200–223.
7. Bonet RP, Nigro N, Storti MA, Idelsohn SR. A discrete non-local (DNL) outgoing boundary condition for diffraction of surface waves. *Communications in Numerical Methods in Engineering* 1998; **14**:849–861.
8. Bonet RP, Nigro N, Storti MA, Idelsohn SR, Condición absorbente discreta no-local (DNL) en diferencias finitas para modelos elípticos de propagación de ondas en el mar. *RIMNE* 1998; **14**(4):481–500.
9. D'Elía J. Numerical methods for the ship wave-resistance problem. *Ph.D. Thesis*, Universidad Nacional del Litoral, Santa Fe, Argentina, 1997 (en español).
10. Kirby JT. A note on parabolic radiation boundary conditions for elliptic wave calculations. *Coastal Engineering* 1989; **13**(3):211–218.
11. Collino F, Monk P. The perfectly matched layer in curvilinear coordinates. *SIAM Journal on Scientific Computing* 1998; **19**:2061–2090.

